Mugla Journal of Science and Technology

BRAIN TUMOR SEGMENTATION ON FLAIR MR IMAGES WITH U-NET

Ercüment GÜVENÇ, Department of Computer Engineering, Süleyman Demirel University, Turkey, eguvenc@mu.edu.tr (https://orcid.org/0000-0003-0053-9623)
Mevlüt ERSOY, Department of Computer Engineering, Süleyman Demirel University, Turkey, mevlutersoy@sdu.edu.tr (https://orcid.org/0000-0003-2963-7729)
Gürcan ÇETİN*, Department of Information Systems Engineering, Muğla Sıtkı Koçman University, Turkey, gcetin@mu.edu.tr (https://orcid.org/0000-0003-3186-2781)

Received: 30.01.2023, Accepted: 18.04.2023 Research Article
*Corresponding author DOI: 10.22531/muglajsci.1244322

Abstract

Brain tumors are among the illnesses that, if not treated promptly, can lead to death. It is extremely difficult to detect tumor tissue using only eye examination methods. As a result, Magnetic Resonance (MR) imaging is used to diagnose brain tumors. T1, T1c, T2, and FLAIR MRI sequences provide detailed information about brain tumors. If the segmentation procedure is performed correctly, patients' chances of survival improve. This paper describes an automated brain tumor segmentation for FLAIR sequences in MR images using U-NeT method. The study has been carried out on the BraTS 2018 data set. The models' correctness has been assessed using the binary accuracy, dice coefficient, and IOU assessment criteria. The results of the comparison between the tumor regions identified by the expert physicians and the tumor regions calculated by the U-Net model are as follows: The model has been completed with 99.26% accuracy, and the Dice Coefficient value, which expresses the similarity on the basis of pixels for the test data, has been found to be 73.99%. Furthermore, the IOU value of 0.59 demonstrated that the model provided accurate estimates for the study.

Keywords: Brain Tumors, Deep Learning, U-Net, Segmentation

U-NET İLE FLAIR MR GÖRÜNTÜLERİNDE BEYİN TÜMÖR BÖLÜTLEMESİ

Özet

Beyin tümörleri, zamanında tedavi edilmediği takdirde ölümle sonuçlanabilecek hastalıklar arasında yer alır. Sadece göz muayenesine dayalı yöntemler ile tümör dokusunu tespit etmek son derece zordur. Bu nedenle, beyin tümörlerini teşhis etmek için Manyetik Rezonans (MR) görüntüleme kullanılır. T1, T1c, T2 ve FLAIR MR sekansları beyin tümörleri hakkında detaylı bilgi vermekte ve bölütleme işlemi doğru yapıldığında hastaların yaşam şansı artmaktadır. Bu makale, U-Net yöntemi kullanılarak MR görüntülerinde FLAIR dizileri için otomatik bir beyin tümörü bulunan bölgelerin bölütlenmesini açıklamaktadır. Bu çalışma, halka açık BraTS 2018 veri seti üzerinde gerçekleştirilmiştir. Modellerin doğruluğu, binary accuracy, dice coefficient ve IOU ölçütleri kullanılarak değerlendirildi. Uzman doktorların tespit ettiği tümör bölgeleri ile U-Net modeli ile tahmin edilen tümör bölgeleri karşılaştırıldığında şu bulgular elde edilmiştir: Model %99.26 doğrulukla tamamlanmış ve benzerliği ifade eden Dice katsayısı değeri test verileri için piksel bazında, %73.99 olarak bulunmuştur. Ayrıca çalışmada IOU değeri 0.59 ile modelin iyi bir tahminde bulunduğunu göstermiştir.

Anahtar Kelimeler: Beyin Tümörleri, Derin Öğrenme, U-Net, Bölütleme

Cite

Güvenç, E., Ersoy M., Çetin G. (2023). "Brain Tumor Segmentation on FLAIR MR Images With U-Net", Mugla Journal of Science and Technology, 9(1), 34-41.

1. Introduction

Brain tumors are classified into four types by the World Health Organization (WHO) based on their location, resemblance to other cells, growth rate, vascularity, and aggressiveness. Low-grade glioma (LGG) refers to grade I and II tumors, whereas high-grade glioma (HGG) refers to grade III and IV tumors [1].

It is challenging to distinguish between normal brain parenchyma and tumor tissue using only visual inspection methods. On the other hand, MRI is widely used in clinics to establish potential diagnoses and available treatments However, due to the unique characteristics of MR data as well as the high variability in tumor sizes or shapes, this remains a very difficult task [2]. The edema region from cerebrospinal fluid can be identified using the FLAIR (Fluid-Attenuated Inversion Recovery) sequence produced by MRI [3].

Accurate brain tumor segmentation from surrounding tissues is a critical step in using FLAIR MRI images in brain tumor research. In the literature, computer-based semi-automatic or fully automated segmentation approaches have been

presented to save clinicians time and eliminate human-based subjectivity [4]. To achieve an effective segmentation result, semi-automated methods still require human interaction, whereas automated systems require anatomical information such as tumor shape, size, regularity, appearance, and localization to build a model and perform the task [5]. In this context, developing a fully automated brain tumor segmentation system remains difficult due to the inability to determine which elements to choose. Machine learning and artificial intelligence techniques have recently been used to address these issues. An automatic brain tumor segmentation model based on the Greedy Snake Model and Fuzzy C-Means (FCM) algorithms was proposed by Sheela and Suganthi [6]. A dataset of T1-weighted contrast images was used for the study. For the glioma, meningioma, and pituitary tumors, the specificity of the suggested method was found to be 0.94, 0.96, and 0.91, respectively. Kalaivani et al. [7] demonstrated the segmentation accuracy of ML classifiers like K-Means, FCM, and K-Nearest Neighbor (K-NN). These classifier algorithms were tested using real-world data from 150 patients from various hospitals. According to the study, K-Means achieved 79.9% accuracy, K-NN achieved 89.96% accuracy, and FCM achieved 98.97% accuracy.

Deep learning techniques, such as CNN networks, have proven to be extremely effective in medical image segmentation [3]. The most popular CNN models are U-Net, SegNet, and ResNet [4]. According to the results of experiments performed on the BraTS2015 dataset, ResNet reduces average calculation time by three times when compared to other DNN approaches, and it has accuracy of 83%, 90%, and 85% for the entire, core, and enhancing regions, respectively [8]. In order to improve tumor segmentation, Alqazzaz et al. [9] investigated SegNet performance. In the study, four separately trained SegNet architectures were merged using post-processing. Dong et al. [10] evaluated the DSC performance of the U-net model using 2D images from the BraTS2015 dataset. The study discovered that 0.88, 0.87, and 0.81 were obtained for HGG and 0.84 and 0.85 for LGG for the entire, core, and enhancing tumor regions, respectively.

This study proposes an automated segmentation method for FLAIR brain tumor images by using the U-Net model. In this study, 155 layers of images from the publicly available multimodal Brain Tumor Segmentation Challenge (BraTS) 2018 dataset were used. The size of the input images in the generated model is determined by the GPU capacity of the computer used, which is 128x128 pixels. The adaptive moment estimation (Adam) algorithm was used to optimize the U-Net model, and the Rectified Linear Unit (ReLU) activation function was used in each learning unit.

The study is divided into the following sections: Section 2 provides technical background on U-Net architecture, evaluation measures, and the dataset. While the proposed models' configuration is explained in Section 3, the test results are evaluated in Section 4.

2. Technical Background

2.1. Auto-encoder

An auto-encoder is designed as a symmetrical artificial neural network which utilizes an unsupervised learning algorithm for efficient data encoding [11, 12]. Auto-encoders having more hidden layers than one can be said to be deep [13]. It is used for size reduction by encoding high-dimensional data with low-dimensional properties.

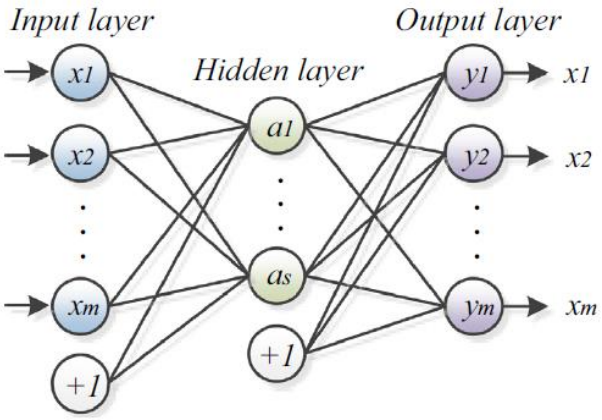

Figure 1. Basic structure of an auto-encoder.

The purpose of an auto-encoder is to ensure that input data is equal to output data [12]. For this purpose, an auto-encoder tries to learn an approximation in the hidden layer so that the input data can be perfectly reconfigured in the output layer [14]. Fig. 1 shows the basic structure of an auto-encoder. Where; the weights of each layer represent different reconstructions of input variables. An auto-encoder must capture the most important features to recover input signals. In addition, by placing restrictions on the network, such as limiting the number or activation of hidden units, the size of inputs can be reduced [13]. If skip connections are removed, U-Net can be considered a type of auto-encoder [11].

2.2. U-Net

A type of architecture called U-Net has been proposed for the semantic segmentation of biomedical images. It is used when it is difficult to access a large number of training images. In order to provide more accurate segmentation and to require fewer training sets, U-net is created by altering the fully connected layer [15]. It is an end-to-end fully convolutional network (FCN), which can accept images of any size because it only has convolutional layers and doesn't have any dense layers.

The original paper states that the U-net architecture has two paths. These components consist of a symmetric expanding path called a decoder and a contraction path called an encoder. Traditional convolutional layers and max pooling layers are used in the encoder to capture context in the image. Transposed convolution method sensitive localization is made possible by decoder. U-net can determine from a picture not only whether or not there is an infection, but also its location.

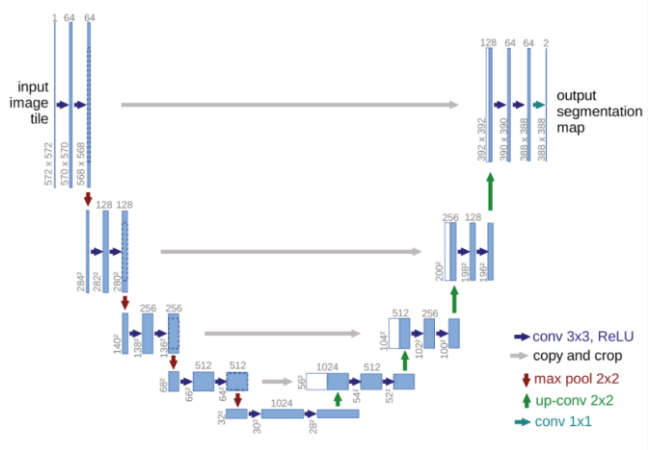

Figure 2. The original U-Net architecture [15].

Since the success of a network depends on both semantic and spatial information, the missing spatial information must be recovered in the segmentation process. This is accomplished by the U-Net network model's decoder, which uses skip links to reassemble higher-resolution feature extractions directly from the encoder using semantic information from the lowest point of the "U"-shaped structure [16]. The architectural layout of the neural network model is depicted in Fig. 2. In accordance with Fig. 2, skip connections are used to combine the feature maps on the left and right. This method allows for the coding-based recovery of lost information. This reduces information loss, particularly in the deeper layers of the coding path for medical images with small target tissues [11].

2.2.1. Activation Functions

DNN models rely heavily on activation functions [16]. It is in charge of converting the weighted input collected in a node into node activation or output for that input. It determines the output of a DNN model, its accuracy, and the computational efficiency of the training process. In this article, the ReLU function is used as an activation function in the output layer between U-Net learning units and the sigmoid function.

With its ease of use and performance, ReLU is a popular activation function. It is a useful function for dealing with gradient vanishing and exploding problems [17, 11]. The output of a ReLU-based layered neural network is always a piecewise linear function of the input [18]. Eq. (1) defines the mathematical expression of ReLU.

$$y_i = \begin{cases} x_i, & if\ x_i > 0 \\ 0, & if\ x_i \leq 0 \end{cases} \quad (1)$$

where xi and yi are the ReLU's input and output. In ReLU, if the input is greater than 0, the output is equal to the input by activating it. When the input is less than 0, the output is set to 0 and is not activated. As a result, the linearity of ReLU is obtained with a constant threshold of 0 [19].

On the other hand, nodes are able to learn more complex data structures thanks to the use of nonlinear activation functions. Sigmoid, also known as the logistic function, is one of the frequently employed nonlinear activation functions. The function converts the input to a number between 0 and 1. Values much smaller than 0 are converted to 0, while inputs significantly larger than 1 are converted to 1. The function has an S-shape from 0 up through 0.5 to 1.0 for all potential inputs. Eq. (2) provides the definition of the sigmoid mathematical expression [20].

$$\sigma(x) = \frac{1}{1 + e^{-x}} \quad (2)$$

2.2.2. Adam Optimizer Algorithm

To ensure a healthy learning process in deep learning applications, the absolute minimum value of the error function must be identified. This procedure is carried out using optimization methods [21]. The Adam algorithm was used to optimize the U-Net model in this article.

Kingma and Ba [22] proposed the Adam algorithm as the main optimization algorithm for large datasets and high dimensional parameters in 2015. It requires little memory and is efficient computationally. Additionally, Adam has a bias redress system. As a result, it makes up for the first minor iteration in which the velocity is biased toward zero when they are started at zero [23]. The Adam optimization algorithm's steps can be outlined as follows [22]:

1. Calculate the gradient g_t at time *t*.
2. Update exponential moving averages of the gradient (m_t) according to the Eq. (3). Where; β1 and β2 are hyper-parameters and control the exponential decay rates of first-order momentum and second-order momentum respectively.

$$m_t = \beta_1 . m_{t-1} + (1 - \beta_1) . g_t \quad (3)$$

3. Update the squared gradient (v_t) according to the Eq. (4).

$$v_t = \beta_2 . v_{t-1} + (1 - \beta_2) . g_t^2 \quad (4)$$

4. Compute bias-corrected first moment estimates according to the Eq. (5). Where; $\widehat{m_t}$ corresponding modifications of the m_t.

$$\widehat{m_t} = \frac{m_t}{(1 - \beta_1^t)} \quad (5)$$

5. Compute bias-corrected second raw moment estimates according to the Eq. (6). Where; $\widehat{v_t}$ corresponding modifications of the $\widehat{v_t}$.

$$\widehat{v_t} = \frac{v_t}{(1 - \beta_2^t)} \quad (6)$$

6. Update parameters according to the Eq. (7). Where; α indicates the learning rate. ε is a very small constant to avoid denominator to be zero [24]

$$\theta_t = \theta_{t-1} - \frac{\alpha . \widehat{m_t}}{\sqrt{\widehat{v_t} + \varepsilon}} \quad (7)$$

It is offered that good default settings for the tested machine learning problems are α = 0.001, β_1 = 0.9, β_2 = 0.999 and ε = 10^{-8} [22, 23].

2.3. Model Evaluation Metrics

This section explains how the methods of Binary Accuracy, Dice Coefficient, and Intersection Over Union (IOU) were used to assess the study's findings.

The Binary Accuracy metric is widely used in image classification, and it represents the percentage of predicted values that match actual values for binary labels [25]. If the probability value is greater than a certain threshold, a 1 value is assigned; otherwise, a 0 value is assigned. It is considered true if the assigned value equals the true value [26].

Dice Coefficient is a similarity measure used to compare two samples. It expresses how much an automatically segmented image overlaps with a manually segmented image as a percentage. 0% indicates no overlap, while 100% indicates perfect overlap [27]. Eq. (8) calculates the Dice Coefficient (similarity) between input set X and output set Y.

$$Dice\ Coefficient = \frac{2\,.\,|X \cap Y|}{|X| + |Y|} \qquad (8)$$

where; |X| and |Y| represent the number of elements in sets X and Y. ∩ is used to show the intersection of X and Y sets. Where *i* and *j* are the positions of the bits on the image; If X_{ij} is equal to Y_{ij}, $|X \cap Y|_{ij}$ become 1, otherwise 0.

IOU is an evaluation metric which divides the area of overlap to total accumulated area for two bounding boxes. The first bounding box (original) is obtain from the labelled training set, while the second bounding box (predicted) is obtain from the trained model. An IOU score greater than 0.5 is generally considered a good estimate [28]. IOU score is calculated with defined in Eq. (9).

$$IOU = \left|\frac{X \cap Y}{X \cup Y}\right| \qquad (9)$$

2.4. Dataset

In general, pre-made data sets are preferred at first when working with medical images. Following the experts' labeling of the images, these data sets are presented to the researchers. The "Multimodal Brain Tumour Segmentation Challenge" dataset from BraTS 2018 is one of them. The data set consists of 3-dimensional brain MR images and tumor labeling in these images. The BraTS2018 training dataset contains 285 3D MR images (210 HGG, 75 LGG), each with four different sequences (T1, T1c, T2, FLAIR). There are segmented images with 155 layers in 240x240 size in the data set designated as the training data set. The deep neural network model created by these images will realize learning. 66 non-segmented test data with identical sequences in the data set are also included [29-33].

3. U-Net Model to Brain Tumor Segmentation

Four steps have been taken to automatically segment brain tumors in MRI FLAIR data using U-Net. Figure 3 depicts the model's overall flowchart. These steps include preprocessing data, training data, testing, and evaluation.

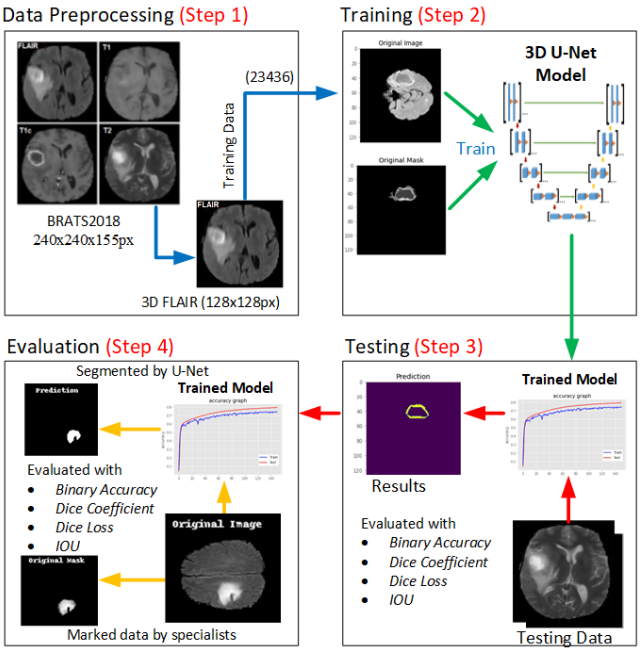

Figure 3. The general flow chart of the proposed system

3.1. Data Preprocessing

In the study, the nibabel library has been used to read and convert data, because the 3D images in the Brats2018 dataset were in nifti format. Thanks to this library, which is used with the Python programming language, 3D patient-based images in 240x240x155 structure have been collected into a different folder together with their tags. All images belonging to 4 different sequences in the dataset have been labelled to match the patient information. The resulting images has been reduced to 128x128 pixels, taking into account the machine GPU capacity to be used during the training phase. The segmentation images corresponding to these images that will be used as input data have been also labelled and reduced to 128x128 pixel in the same way. In the study, 23436 of 32550 images of 128x128 pixels belonging to 210 patients in the FLAIR sequence were reserved for training, 5859 for validation and 3255 for testing.

3.2. U-Net Model

The architecture used in the study consists of 4 block levels. Each block has 2 CNN layers with ReLU activation function, and the encoder section contains maxpooling layers. In the decoding section, they were replaced by up-CNN layers.

In the offered model, the input data is set to 128x128 pixels, and the batch size value was also set to 16 due to the GPU limitation of the computer where the training was taking place (Intel i7-8550, 8GB Ram, NVIDIA GeForce930 MX). In addition, the number of CNN layer filters in each block was set at 16, 32, 64, and 128. The layer in the lowest block has 256 filters. From the encoder layers, connections were made to the layers corresponding to the decoder sections. Clipping was required due to the loss of edge pixels in each evolution. In the last layer, the 1x1 convolution was used to map each 64-component property vector to the desired number of classes.

The performance of the U-Net model, as with other deep learning methods, depends largely on the optimum values of the hyper parameters used. Hyper parameter refers to all parameters of a model used to achieve the best accuracy. They cannot be updated at the learning stage. In the study, Training parameters were changed and updated manually to achieve the best results. Since the performance and loss values of the offered model did not change significantly after 150 epoch, it was selected as 150.

The model was trained by using the Adam optimization algorithm with a learning rate of 0.001. ReLU activation function was chosen among the layers, since it is efficient to gradient vanishing and exploding problems. Moreover, the sigmoid activation function was used in the output layer.

4. Experimental Results and Discussion

Fig. 4 and Fig. 5 display the changes in accuracy and loss values during the duration of the model's training. Fig. 4 shows training and testing success, whereas Fig. 6 shows training and testing loss. The total number of errors produced for each instance in the training or validation sets is called loss. The loss value indicates how well or poorly a model performs after each optimization cycle. Training was limited to 150 epochs since there was no significant cost reduction and no gain in success after 150 epochs. The decrease in training loss over time indicates that the model is well-suited to the dataset. Training and test accuracy values increase almost simultaneously, while training and test loss values fall and continue to decrease at the same time, indicating that the model is not overfitting.

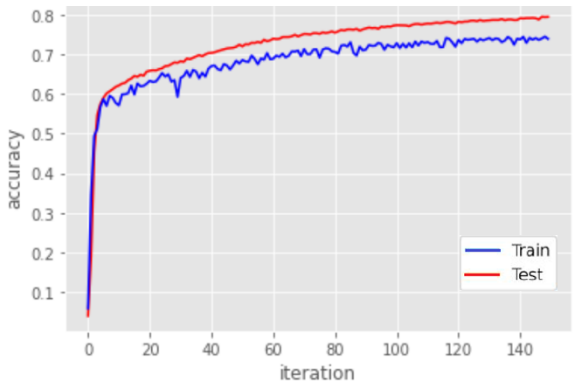

Figure 4. The accuracy performance of the U-Net model.

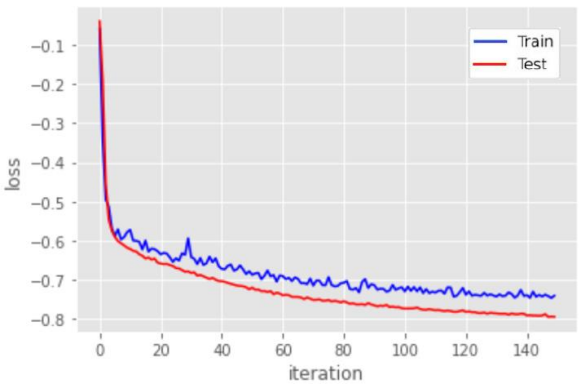

Figure 5. The loss performance of the U-Net model.

The model's accuracy was measured using Binary Accuracy, Dice Coefficient, and IOR assessment metrics. Table 1 below shows the performance results for 3255 test data.

Table 1. Test data performance results.

Binary Accuracy	Dice Loss	Dice Coefficient	IOU
0.9979	*-0.7533*	*0.7513*	*0.6238*

Table 1 shows that the generated model's training was finished with 99 percent accuracy. Furthermore, the Dice Coefficient value, which refers to the similarity of test results on a pixel basis, was 73.95 percent. The value of the IOU was discovered to be 0.6238. If the IOU value is more than 0.5, the model is making a good prediction.

The identification of the tumor location for test data was done with extremely good accuracy utilizing only FLAIR images, according to the results obtained from the assessment criteria. Fig. 6 shows several sample pictures of the actual tumor region and the tumor regions predicted using the U-Net model, based on the test results.

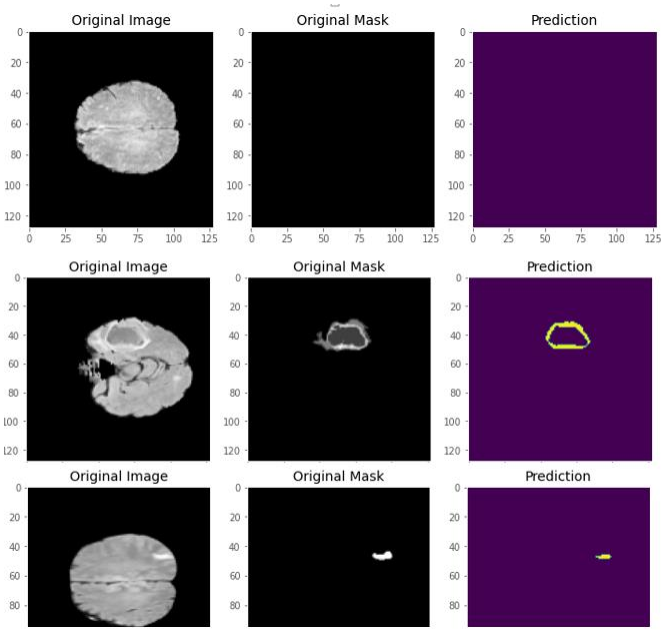

Figure 7. Tumor regions estimated with the U-Net model.

The FLAIR images from 14 of the 66 test results were analyzed in the BraTS 2018 dataset using expert physicians and the areas of tumors were identified. Table 2 shows the results of comparing the images of the tumor region identified by the expert physicians with the tumor regions predicted by the U-Net model.

Fig. 7 shows several sample images of marked tumor regions by specialists and predicted tumor regions using the U-Net model, based on Table 2 results.

Table 2. Results of comparing tumor regions

Binary Accuracy	Dice Loss	Dice Coefficient	IOU
0.9926	*-0.8457*	*0.7399*	*0.592 2*

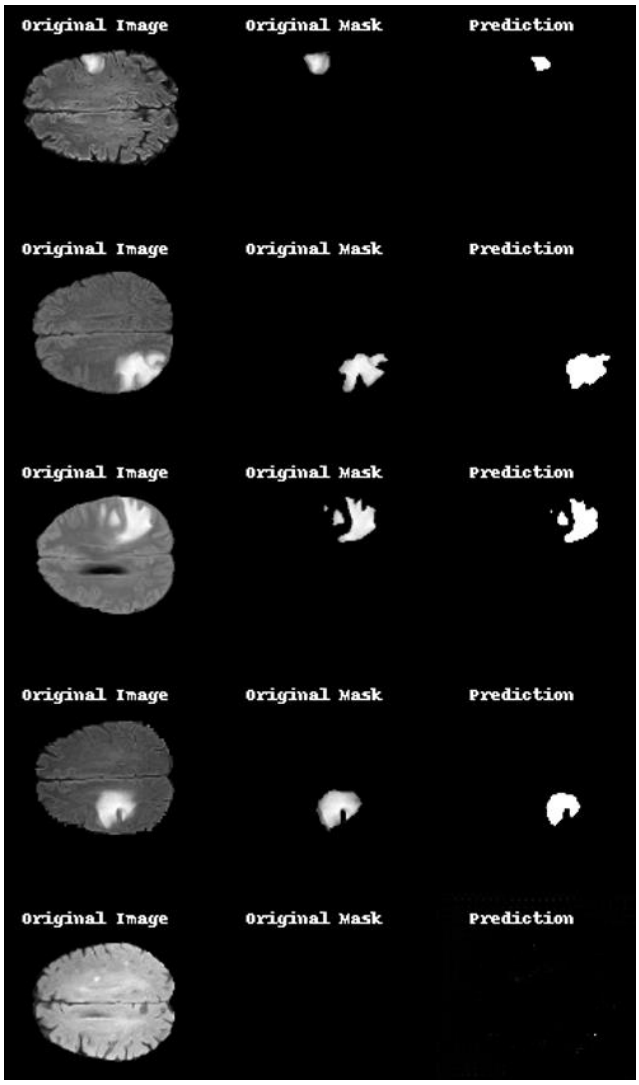

Figure 7. Tumor regions estimated from the U-Net model and marked by specialist doctors.

Table 3 shows a comparison of the proposed approach to the literature. Demir et al [34] proposed a method for segmenting 3D MRI images based on a deep learning strategy. The 3D Attention Convolutional LSTM (3ACL) model was used in the study to extract deep features from MRI data using the sequences T1, T1gd, T2, FLAIR. The weighted majority was then used to improve the model's overall performance. The accuracy of the SVM algorithm, which provides the best performance in the weighted majority process, was 98.90% (BRATS2015) and 99.29% (BRATS2016) (BRATS2018). Mzoughi et al [34] classified HGG and LGG using the CNN method. On 3D MR images, the method achieved 96.49% accuracy using T1gd sequences. Pedada et al [36], on the other hand, attempted to improve overall performance by replacing the encoder of the classical U-Net model with that of a ResNet-34 model. On the BRATS 2018 dataset, it achieved 92.20% accuracy and 0.854 dice score. A study was conducted on the BRATS 2020 dataset, comparing the MM-Link-Net model proposed by Ramasamy et al [37] with SeNet and U-Net deep learning methods. The multi-modal MRI features are fused together in the sudy and fed into an encoder-decoder based LinkNet Architecture. The backbone discriminator architecture for segmentation is a pre-trained ResNET152 architecture. Only FLAIR images were the subject of Zeineldin et al's [38] study. A DeepSeg Framefork with various deep learning models has been created for this purpose. With an average DS value ranging from 0.80 to 0.83, the proposed deep learning architectures were successful in detecting tumor regions in the validation set. Jwaid et al. [39] suggested a new U-Net architecture to increase 3D MRI image detection performance. The upper/lower sampling module in the new U-Net architecture has been altered by the removal of the upper/layer pooling layer from the original U-Net architecture. Although the new U-Net model requires more training time, it outperformed the SegNet5 architecture with 98.9% accuracy and 0.69 IoU values. The proposed study, like the studies of Mzoughi et al [34] and Zeineldin et al [38], focuses on a single sequence (FLAIR) and 2D images rather than the model. The main goal here is to demonstrate that high-performance segmentation can be accomplished on 2D images by reducing the amount of high-dimensional data in

Table 3. Comparison of proposed method with state-of-the-art methods

Ref	Authors	Segmentation	Dataset	Metrics (Acc, DS, IoU)	Modalities
[34]	Demir et al (2023)	3ACL, Weighted Majority (SVM)	BRATS 2015, BRATS 2018	98.90% (Acc) 99.29% (Acc)	T1, T1gd, T2, FLAIR
[35]	Mzoughi et al (2020)	CNN	BRATS 2018	96.49% (Acc)	T1gd
[36]	Pedada et al (2023)	Modified U-Net	BRATS 2017, BRATS 2018	93.40% (Acc), 0.821 (DS) 92.20% (Acc), 0.854 (DS)	T1, T1gd, T2, FLAIR,
[37]	Ramasamy et al (2023)	MM-Link-Net SeNet U-Net	BRATS 2020	0.777 (DS) 0.7320 (DS) 0.75 (DS)	T1, T1gd, T2, FLAIR,
[38]	Zeineldin et al (2020)	UNet, Modified U-Net, VGGNet, ResNet, DenseNet	BRATS 2019	0.80 (DS) 0.81 (DS) 0.83 (DS) 0.81 (DS) 0.83 (DS)	FLAIR
[39]	Jwaid (2021)	3D U-Net CNN, SegNet5	BRATS 2017	98.9% (Acc), 0.69 (IoU) 96.2% (Acc), 0.55 (IoU)	T1, T1gd, T2, FLAIR,
	Proposed model	2D U-Net	BRATS 2018	99.26% (Acc), 73.99 (DS), 0.59 (IoU)	FLAIR

the 3D structure. The study's accuracy, DS, and IoU values support the literature studies, taking into account the parameters used in the U-Net model's training.

5. Conclusion

A U-Net model for 3D brain tumor detection and segmentation is given in this study. In this investigation, 155 layers of images from the publically accessible multimodal BraTS2018 dataset containing solely the FLAIR MRI were utilized. The major objective for this is to see how well the tumor region can be segmented using the U-net deep learning approach using only one sequence type from multimodal MRI data. Thus, it has been demonstrated to what extent the performance rate of data with only one sequence can change in environments where the ready data set is not used and proper records cannot be obtained. According to the results of the study; the model created was completed with 99.26% accuracy, 73.99 Dice Coefficient value, and 0.5922 IOU value. The findings demonstrate that the model is generating an accurate prediction.

This investigation concentrated on raw FLAIR images. In other words, there has been no image processing performed to the FLAIR images. Pre-processing techniques on the image can improve the work's accuracy. Moreover, it is possible to add dense module, inception module and etc. to the encoding path of the U-Net model. The effects of the improvements will also be explored in future studies.

Notes

This paper is resulted from the doctoral (PhD) thesis study of the first author.

6. References

[1] Chen, H., Qin, Z., Ding, Y., and Qin Z., "Brain tumor segmentation with deep convolutional symmetric neural network", *Neurocomputing*, vol. 392, pp. 305-313, 2020.

[2] Lorenzo, P. R., Nalepa, J., Billewicz, B. B., Wawrzyniak, P., et al. " Segmenting brain tumors from FLAIR MRI using fully convolutional neural networks", *Computer Methods and Programs in Biomedicine*, vol. 176, pp. 135-148, 2019.

[3] Daimary, D., Bora, M. B., Amitab, K., and Kandar, D., "Brain Tumor Segmentation from MRI Images using Hybrid Convolutional Neural Networks", *International Conference on Computational Intelligence and Data Science*, 2019.

[4] Zeineldin, R. A., Karar, M. E., Coburger, J., Wirtz, C. R., and Burgert, O., "DeepSeg: deep neural network framework for automatic brain tumor", *International Journal of Computer Assisted Radiology and Surgery*, vol. 15, pp. 909-920, 2020.

[5] Wadhwa, A., Bhardwaj, A., and Verma, V. S., "A review on brain tumor segmentation of MRI images", *Magnetic Resonance Imaging*, vol. 61, pp. 247–259, 2019.

[6] Sheela, C. J. J., and Suganthi, G., "Automatic Brain Tumor Segmentation from MRI using Greedy Snake Model and Fuzzy C-Means Optimization", *Journal of King Saud University – Computer and Information Sciences*, pp. 1-10, 2019.

[7] Kalaivani, I., Oliver, A. S., Pugalenthi, R., Jeipratha, P. N., Jeena, A. A. S., and Saranya, G., "Brain Tumor Segmentation Using Machine Learning Classifier", *Fifth International Conference on Science Technology Engineering and Mathematics*, 2019.

[8] Shehab, L. H., Fahmy, O. M., Gasser, S. M., and El-Mahallawy, M. S., "An efficient brain tumor image segmentation based on deep residual networks (ResNets)", *Journal of King Saud University – Engineering Sciences*, 2020.

[9] Alqazzaz, S., Sun, X., Yang, X., and Nokes, L., "Automated brain tumor segmentation on multi-modal MR image using SegNet", *Computational Visual Media*, vol. 5(2), pp. 209–219, 2019.

[10] Dong, H., Yang, G., Liu, F., Mo, Y., and Guo, Y., "Automatic Brain Tumor Detection and Segmentation *Using U-Net Based Fully Convolutional Networks", Medical Image Understanding and Analysis*, 2017.

[11] Li, S., Tso, G. K., and He, K., "Bottleneck feature supervised U-Net for pixel-wise liver and tumor segmentation", *Expert Systems with Applications*, vol. 145, pp. 1-11, 2020.

[12] Zhang, Y., Zhang, E., and Chen, W., "Deep neural network for halftone image classification based on sparse auto-encoder", *Engineering Applications of Artificial Intelligence*, vol. 50, pp. 245-255, 2016.

[13] Liu, T., Li, Z., Yu, C., and Qin, Y., "NIRS feature extraction based on deep auto-encoder neural network", *Infrared Physics & Technology*, vol. 87, pp. 124-128, 2017.

[14] Sun, W., Shao, S., Zhao, R., Yan, R., Zhang, X., and Chen, X., "A sparse auto-encoder-based deep neural network approach for induction motor faults classification", *Measurement*, vol. 89, pp. 171-178, 2016.

[15] Ronneberger, O., Fischer, P., and Brox, T., "U-Net: Convolutional Networks for Biomedical Image Segmentation", *Medical Image Computing and Computer-Assisted Intervention – MICCAI* 2015, pp. 234-241, Munich, 2015.

[16] F. Isensee, P. Kickingereder, W. Wick, M. Bendszus and K. H. Maier-Hein, "No New-NET", *Brainlesion: Glioma, Multiple Sclerosis, Stroke and Traumatic Brain Injuries*, no. 11384, pp. 234-244, 2019.

[17] E. Hussain, H. Mahmudul, M. Anisur Rahman, I. Lee, T. Tamanna and M. Zavid Parvez, "CoroDet: A deep learning based classification for COVID-19 detection using chest X-ray images", *Chaos, Solutions & Fractals*, vol. 142, pp. 1-12, 2021.

[18] K. Eckle and J. Schmidt-Hieber, "A comparison of deep networks with ReLU activation function and linear spline-type methods", *Neural Networks*, vol. 110, pp. 232-242, 2019.

[19] J. Cao, Y. Pang, X. Li and J. Liang, "Randomly translational activation inspired by the input

distributions of ReLU", *Neurocomputing*, vol. 275, pp. 859-868, 2018.

[20] J. Brownlee, "A Gentle Introduction to the Rectified Linear Unit (ReLU)", 2019. [Online]. Available: https://machinelearningmastery.com/rectified-linear-activation-function-for-deep-learning-neural-networks/. [Accessed 25 8 2022].

[21] G. Ser and C. T. Bati, "Determining the Best Model with Deep Neural Networks: Keras Application on Mushroom Data", *YYU Journal of Agricultural Science*, vol. 29, no. 3, pp. 406-417, 2019.

[22] D. P. Kingma and J. L. Ba, "Adam: A Method for Stochastic Optimization", *in International Conference on Learning Representations*, 2015.

[23] S. Remya and R. Sasikala, "Performance evaluation of optimized and adaptive neuro fuzzy inference system for predictive modeling in agriculture," *Computers & Electrical Engineering*, vol. 86, pp. 1-14, 2020.

[24] Z. Fei, Z. Wu, Y. Xiao, J. Ma and W. He, "A new short-arc fitting method with high precision using Adam optimization algorithm", *Optik*, vol. 212, pp. 1-7, 2020.

[25] W. Siguerdidjane, F. Khameneifar and F. P. Gosselin, "Efficient planning of peen-forming patterns via artificial neural networks", *Manufacturing Letters*, vol. 25, pp. 70-74, 2020.

[26] G. Dommaraju, "Keras' Accuracy Metrics. Understand them by running simple experiments in Python," [Online]. Available: https://towardsdatascience.com/keras-accuracy-metrics-8572eb479ec7. [Accessed 15 11 2022].

[27] H. Kumar, S. V. DeSouza and M. S. Petrow, "Automated pancreas segmentation from computed tomography and magnetic resonance images: A systematic review", *Computer Methods and Programs in Biomedicine*, vol. 178, pp. 319-328, 2019.

[28] M. S. ul Islam, "Using deep learning based methods to classify salt bodies in seismic images", *Journal of Applied Geophysics*, vol. 178, pp. 1-9, 2020.

[29] S. Bakas, H. Akbari, A. Sotiras, M. Bilello and M. Rozycki, "Segmentation labels and radiomic features for the preoperative scans of the tcga-gbm collection", *Cancer Imaging Arc.*, vol. 286, 2017.

[30] S. Bakas, H. Akbari, A. Sotiras, M. Bilello, M. Rozycki and J. a. Kirby, "Advancing The Cancer Genome Atlas glioma MRI collections with expert segmentation labels and radiomic features", *Nature Scientific Data*, 2017.

[31] S. Bakas, H. Akbari, A. Sotiras, M. Bilello and e. al., "Segmentation labels and radiomic features for the preoperative scans of the tcga-lgg collection", *The Cancer Imaging Archive*, 2017. [Online].

[32] S. Bakas, M. Reyes, A. Jakab, S. Bauer, M. Rempfler, A. Crimi and e. al., "Identifying the Best Machine Learning Algorithms for Brain Tumor Segmentation, Progression Assessment, and Overall Survival Prediction in the BRATS Challenge," arXiv:1811.02629, 2018.

[33] B. H. Menze, A. Jakab, S. Bauer, J. Kalpathy-Cramer, K. Farahani and J. Kirby, "The Multimodal Brain Tumor Image Segmentation Benchmark (BRATS)", *IEEE Transactions on Medical Imaging*, vol. 34, no. 10, pp. 1993-2024, 2015.

[34] F. Demir, Y. Akbulut, B. Taşcı and K. Demir, "Improving brain tumor classification performance with an effective approach based on new deep learning model named 3ACL from 3D MRI data", *Biomedical Signal Processing and Control*, vol.81, 2023.

[35] H. Mzoughi, I. Njeh, A. Wali, M. B. Slima, A. B. Hamida, C. Mhiri and K. B. Mahfoudhe, "Deep Multi-Scale 3D Convolutional Neural Network (CNN) for MRI Gliomas Brain Tumor Classification", *Journal of Digital Imaging*, vol. 33, pp. 903–915, 2020.

[36] K. R. Pedada, R. A. Bhujanga, K. K. Patro, J. P. Allam, M. M. Jamjoom, N. A. Samee, " A novel approach for brain tumour detection using deep learning based technique", *Biomedical Signal Processing and Control*, vol. 82, 2023.

[37] G., Ramasamy, T. Singh, X. Yuan, "Multi-Modal Semantic Segmentation Model using Encoder Based Link-Net Architecture for BraTS 2020 Challenge", *Procedia Computer Science*, vol. 218, pp. 732-740, 2023.

[38] R. A. Zeineldin, M. E. Karar, J. Coburger, C. R. Wirtz, O. Burgert, "DeepSeg: deep neural network framework for automatic brain tumor segmentation using magnetic resonance FLAIR images", *International Journal of Computer Assisted Radiology and Surgery*, vol. 15, pp. 909-920, 2020.

[39] W. M. Jwaid, Z. S. Al-Husseini, A. H. Sabry, "Development of Brain Tumor Segmentation of Magnetic Resonance Imaging (MRI) Using U-Net Deep Learning", *Eastern-European Journal of Enterprise Technologies*, vol. 4(9), pp. 23-31, 2021.